Supplement of Atmos. Chem. Phys., 22, 13167–13182, 2022
https://doi.org/10.5194/acp-22-13167-2022-supplement

Atmospheric Chemistry and Physics Open Access

Supplement of

Particle-phase processing of α-pinene NO_3 secondary organic aerosol in the dark

David M. Bell et al.

Correspondence to: David M. Bell (david.bell@psi.ch) and Claudia Mohr (claudia.mohr@aces.su.se)

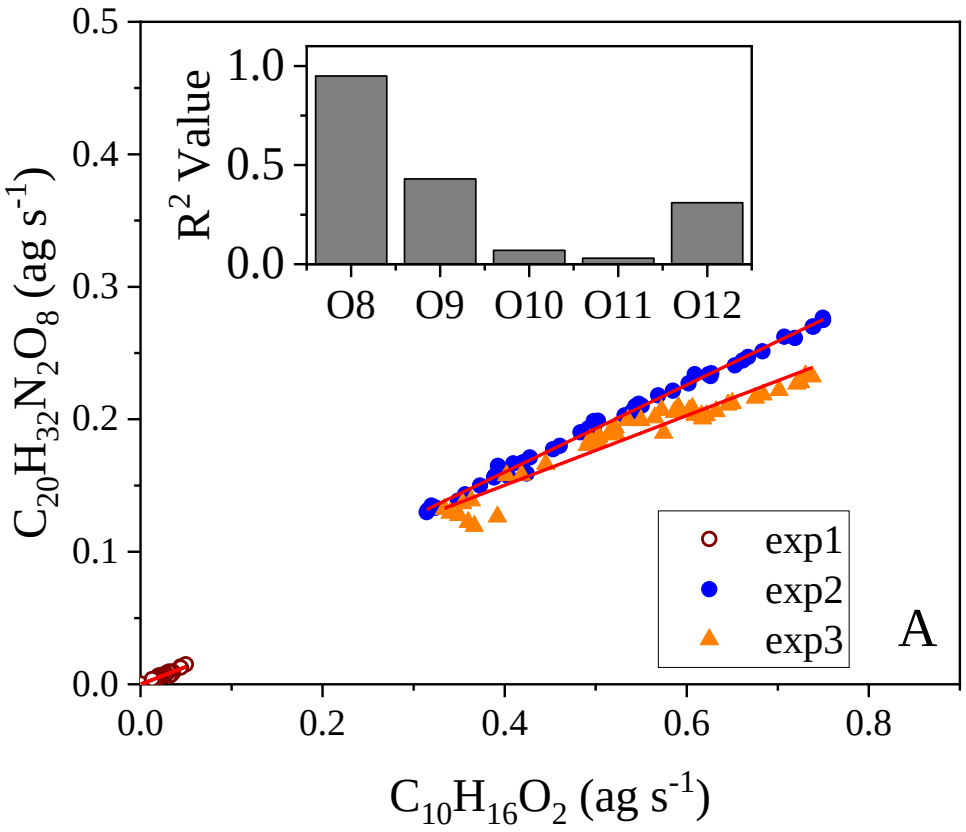

Figure S1: Correlation plot of $C_{10}H_{16}O_2$ and $C_{20}H_{32}N_2O_8$. (inset) R^2 values for the comparison between $C_{10}H_{16}O_2$ and the series of $C_{20}H_{32}N_2O_x$ (x = 8 – 12).

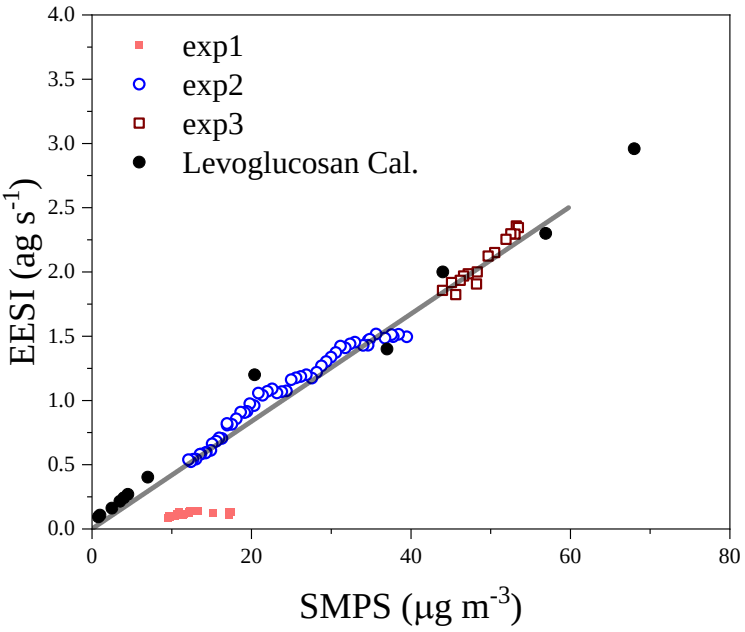

Figure S2: EESI mass flux compared to the measured SMPS mass for experiments 1 – 3, when the EESI was present. The total mass flux measured by the EESI is the ion signal (s^{-1}) converted to measured mass per second by scaling each molecular formula according to its mass. The levoglucosan calibration curve was added for the period where the EESI was fully operational (Exp 2 and 3).

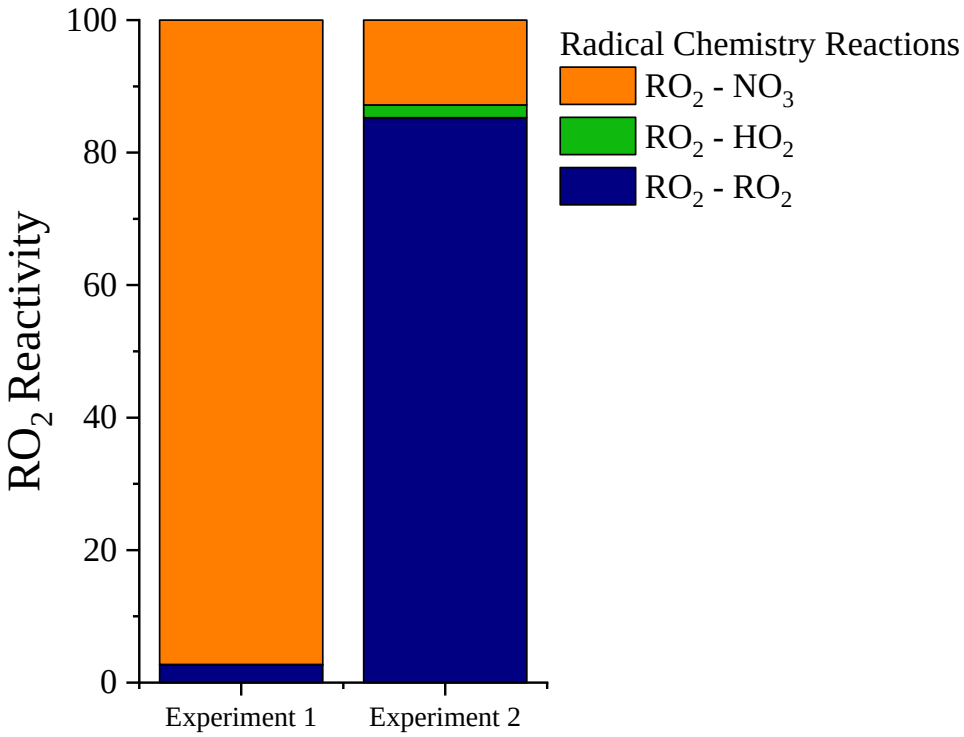

Figure S3: Integrated radical reactivity of RO_2 radicals in experiment 1 and experiment 2 modeled with the Master Chemical Mechanism (MCM) (Jenkin et al., 2003; Saunders et al., 2003). The absolute values will differ depending on the reaction rates of $RO_2 – RO_2$, but this provides insight into the reactions controlling the initial composition of the particle phase.

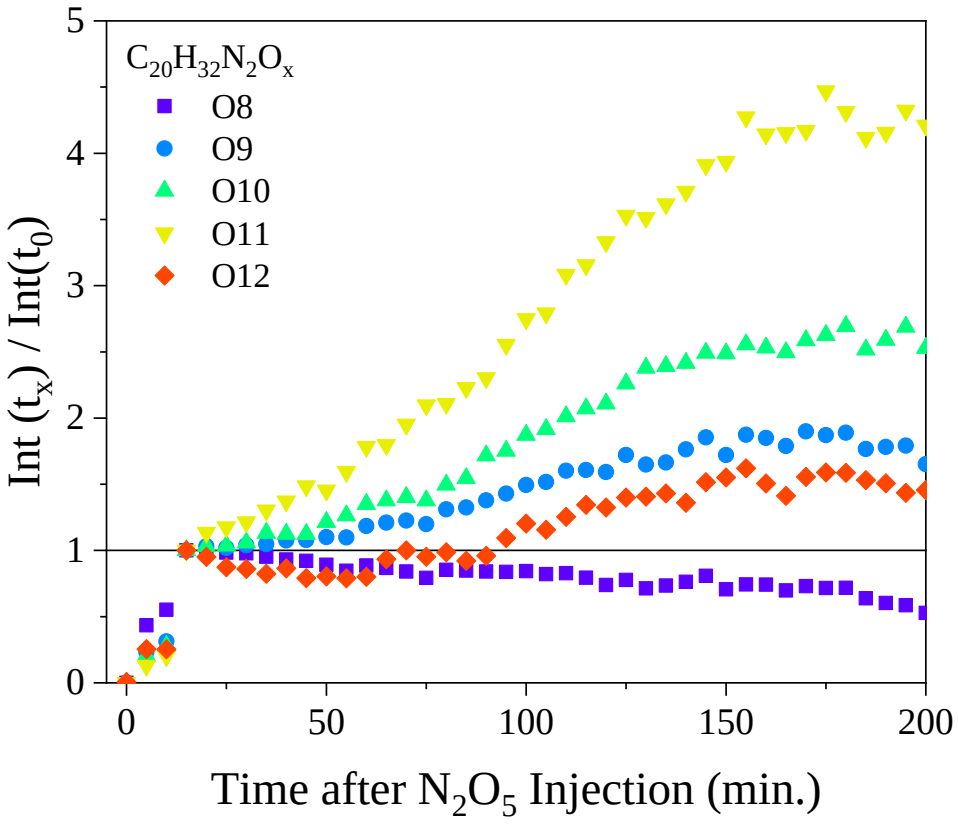

Figure S4: Normallized $C_{20}H_{32}N_2O_x$ dinitrate signals relative to *t* = 15 min mass from experiment 3. *t* = 15 min represents the maximum in particle mass, which is why this time was chosen.

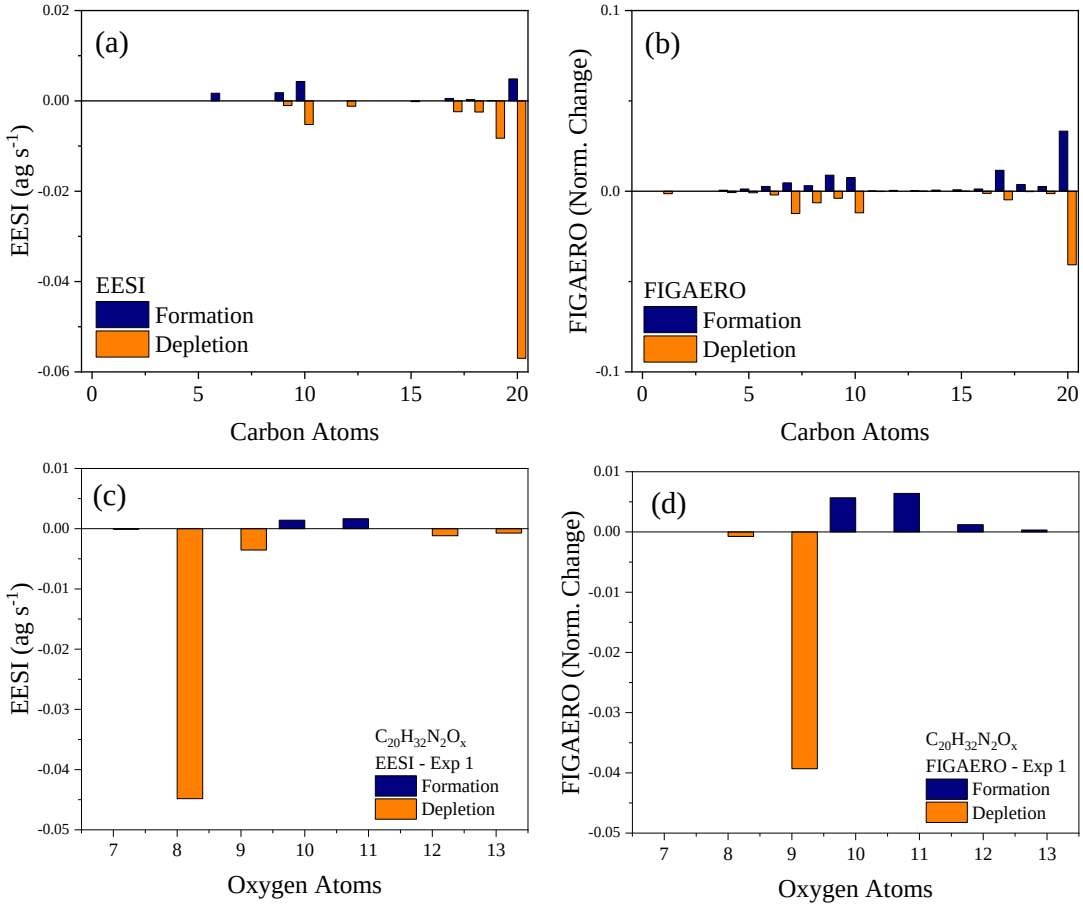

Figure S5: (a) and (b) Carbon distribution of the molecules formed (blue) and depleted (orange) in the particle phase during aging for both the EESI **(a)** and FIGAERO-CIMS **(b)**, respectively for exp 1. (**c & d)** The change in the oxygen distribution for the $C_{20}H_{32}N_2O_{8\text{-}13}$ molecules during dark aging for the EESI-ToF **(c)** and FIGAERO-CIMS **(d)**, respectively.

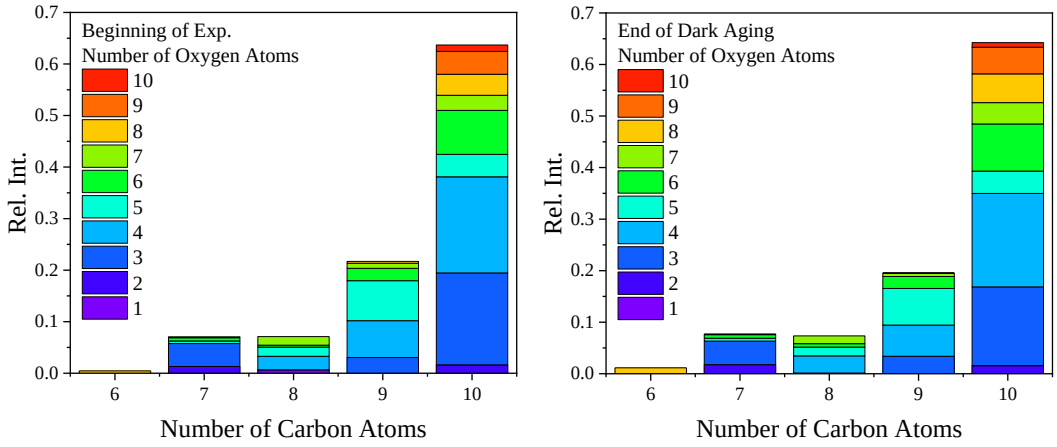

Figure S6: Monomer carbon and oxygen atom distribution for the beginning of the experiment t_{early} = 10 min and end of dark aging t = 240 min for exp 2.

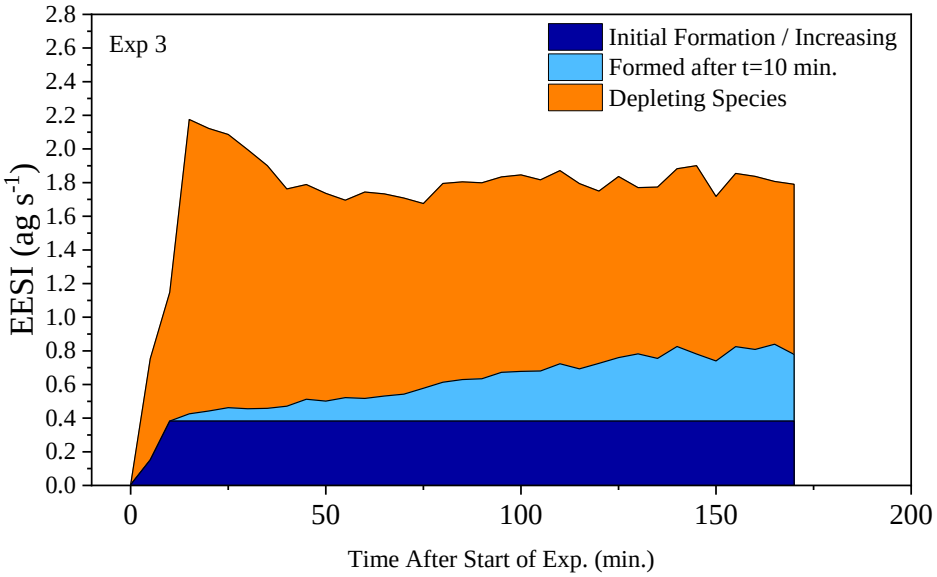

Figure S7: Total EESI-ToF intensity plotted as a function of the contribution from different sources, particle phase formation products determined from those molecular formula that increase during dark aging after t = 10 min, while those decreasing are shown in orange. The data is shown for experiment 3. The species forming in the dark are split into the dark blue (intensity at t = 15 min) and the fraction increasing after that time in light blue.

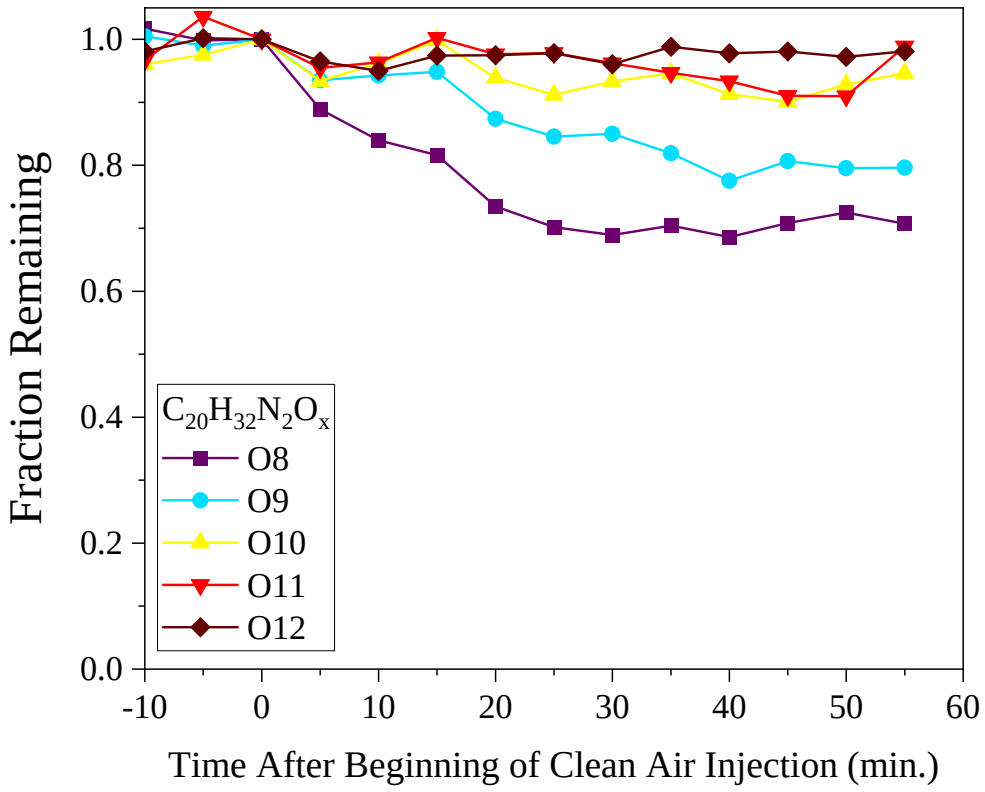

Figure S8: After experiment 3, clean air was injected into the chamber at 100 L min^{-1} for 60 min. The time traces here correspond to the EESI-ToF intensity relative to the time at the beginning of the injection of clean air into the chamber for the series of $C_{20}H_{32}N_2O_{8\text{-}12}$.

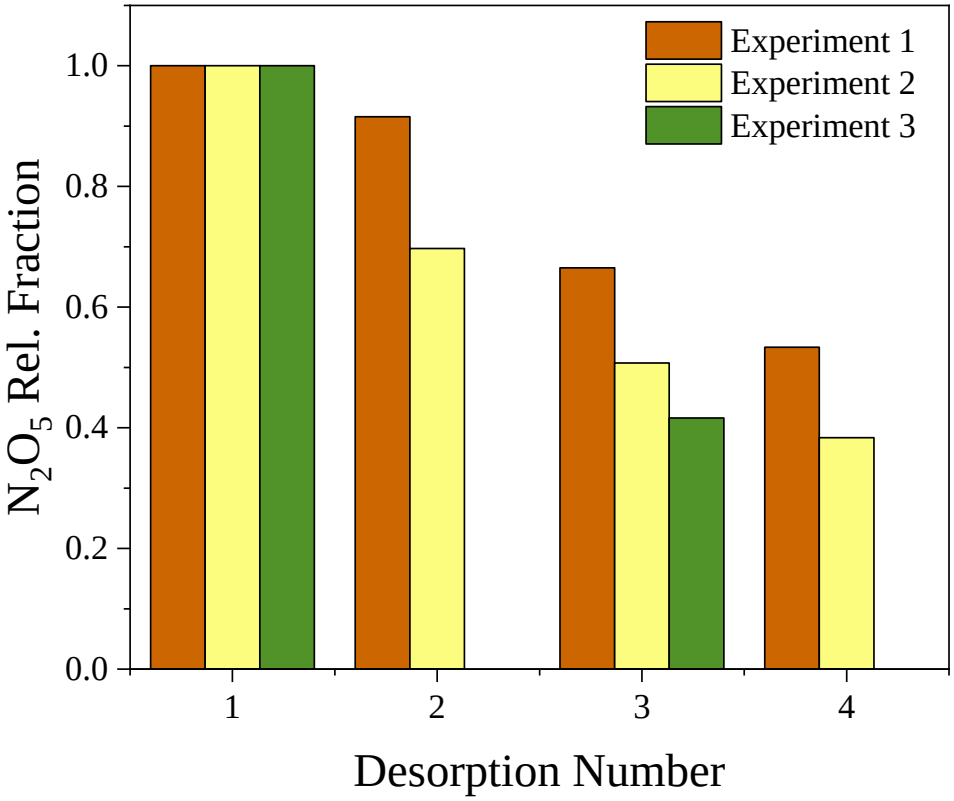

Figure S9: N_2O_5 particle phase relative fraction normalized to the initial desorption measured by the FIGAERO-CIMS. Estimated mass concentrations in the particle phase are 0.03 – 0.06 μg m^{-3}. The time between each desorption was about 1-1.5 h.

References:

Jenkin, M. E., Saunders, S. M., Wagner, V., and Pilling, M. J.: Protocol for the development of the Master Chemical Mechanism, MCM v3 (Part B): tropospheric degradation of aromatic volatile organic compounds, Atmos. Chem. Phys., 3, 181-193, 2003, 10.5194/acp-3-181-2003.
Saunders, S. M., Jenkin, M. E., Derwent, R. G., and Pilling, M. J.: Protocol for the development of the Master Chemical Mechanism, MCM v3 (Part A): tropospheric degradation of non-aromatic volatile organic compounds, Atmos. Chem. Phys., 3, 161-180, 2003, 10.5194/acp-3-161-2003.